Differential Resting-State Functional Connectivity of Striatal Subregions in Bipolar Depression and Hypomania

Murat I. Altinay,[1] Leslie A. Hulvershorn,[1,2] Harish Karne,[1,2] Erik B. Beall,[3] and Amit Anand[1,2]

Abstract

Bipolar disorder (BP) is characterized by periods of depression (BPD) and (hypo)mania (BPM), but the underlying state-related brain circuit abnormalities are not fully understood. Striatal functional activation and connectivity abnormalities have been noted in BP, but consistent findings have not been reported. To further elucidate striatal abnormalities in different BP states, this study investigated differences in resting-state functional connectivity of six striatal subregions in BPD, BPM, and healthy control (HC) subjects. Ninety medication-free subjects (30 BPD, 30 BPM, and 30 HC), closely matched for age and gender, were scanned using 3T functional magnetic resonance imaging (fMRI) acquired at resting state. Correlations of low-frequency blood oxygen level dependent signal fluctuations for six previously described striatal subregions were used to obtain connectivity maps of each subregion. Using a factorial design, main effects for differences between groups were obtained and *post hoc* pairwise group comparisons performed. BPD showed increased connectivity of the dorsal caudal putamen with somatosensory areas such as the insula and temporal gyrus. BPM group showed unique increased connectivity between left dorsal caudate and midbrain regions, as well as increased connectivity between ventral striatum inferior and thalamus. In addition, both BPD and BPM exhibited widespread functional connectivity abnormalities between striatal subregions and frontal cortices, limbic regions, and midbrain structures. In summary, BPD exhibited connectivity abnormalities of associative and somatosensory subregions of the putamen, while BPM exhibited connectivity abnormalities of associative and limbic caudate. Most other striatal subregion connectivity abnormalities were common to both groups and may be trait related.

Key words: bipolar disorder; connectivity; resting state; striatum

Introduction

BIPOLAR DISORDER (BP) IS a major mental illness with hallmark mood states of (hypo)mania (BPM) and depression (BPD). However, differences in brain function between these mood states are still unclear and remain critical to our understanding of the pathophysiology of BP. Thus, to investigate the pathophysiology of BP, different phases of the disorder must be compared with healthy subjects (healthy control [HC]) and also with each other.

Although classically considered as motor structures (Kemp and Powell, 1971), the basal ganglia, especially the striatum (i.e., putamen and the caudate), are also essential to the regulation of cognition and emotion (Goldman and Nauta, 1977; Kunzle, 1975; Townsend and Altshuler, 2012). An amygdala–

striato–pallido–thalamic–cortical circuit has been identified as a core circuit involved in mood generation and regulation (Price and Drevets, 2010). The striatum is a critical node in this circuit as it communicates with the cortex and thalamus, as well as limbic areas such as the amygdala. A number of studies have reported task-induced and functional connectivity abnormalities of the striatum in BP and a number of excellent reviews are available (Phillips and Swartz, 2014; Strakowski et al., 2005; Vargas et al., 2013; Wessa et al., 2014). However, as mentioned above, few studies have concurrently compared BPM and BPD.

To date, there have been no consistent reported findings in task-induced functional magnetic resonance imaging (fMRI) studies in different states of BP. In their comprehensive review, Marchand and Yurgelun-Todd (2010) reported that

---

[1]Center for Behavioral Health, Cleveland Clinic, Cleveland, Ohio.
[2]Department of Psychiatry, Indiana University School of Medicine, Indianapolis, Indiana.
[3]Imaging Institute, Cleveland Clinic, Cleveland, Ohio.

studies that investigated striatal activation in bipolar mania showed increased ventral striatum and caudate activity in response to motor (simple reaction time test) and emotional (alternating blocks of captioned pictures) tasks. Similar activation results were reported in studies that investigated motor and emotional tasks in BPD. For euthymic BP, however, the studies reported increased striatal activity in response to motor and cognitive tasks and decreased striatal activity in response to emotional tasks. Despite the inconsistency, these different activation patterns in different phases of BP suggest that these findings may represent state-related differences.

Resting-state functional connectivity studies in BP have also reported striatal connectivity abnormalities in BP. Anand and colleagues (2009) reported decreased pregenual anterior cingulate cortex (pgACC) connectivity with left pallidostriatum in both BPD and BPM. Teng and colleagues (2014) recently reported decreased connectivity in the striatal–thalamic circuit and between the striatal regions and the middle and posterior cingulate cortex for resting-state connectivity in BP versus HC.

However, until the present time, a reliable pattern of striatal activation and connectivity abnormality in BP has not emerged. One reason may be that these studies have not taken into account the structural and functional diversity of the striatum. Alexander and colleagues (1986) described five functionally distinct loops involving different striatal subregions and postulated a dissociative connectivity of the caudate and putamen regions to cortical areas based on a dorsal/ventral and rostral/caudal divide. Through this work, and the work of several other investigators, based on the pattern of connectivity with the cortical regions, the striatum has been divided into (1) associative striatum (dorsal caudate [DC] and rostral putamen), which connects putamen as well as body and tail of caudate nucleus to associative cortices in the frontal, temporal, and parietal lobes (Carpenter, 2011; Goldman and Nauta, 1977; Kunzle, 1975; Ragsdale and Graybiel, 1981); (2) sensorimotor striatum, which connects dorsolateral putamen and the dorsolateral rim of the head of the caudate nucleus to motor and somatosensory cortices (DeLong and Georgopoulos, 2011; Kunzle, 1975; Liles and Updyke, 1985); and (3) limbic striatum (ventral striatum inferior [VSI] and ventral striatum superior [VSS]), which connects most ventral parts of both the caudate nucleus and the putamen to limbic and paralimbic cortices, amygdala, and the hippocampus (Alheid and Heimer, 1988; Berendse et al., 1992; Haber et al., 1990; Phelps and Vaughn, 1986; Russchen et al., 1985).

More recently, Postuma and Dagher (2006) used a meta-analysis of fMRI task-induced activation studies to validate these subdivisions. Furthermore, Di Martino and colleagues (2008), using resting-state connectivity paradigm in healthy subjects, investigated the connectivity of six striatal subregions, including three caudate regions (DC), VSS, and VSI and three putamen regions (dorsal rostral putamen [DRP], dorsal caudal putamen [DCP], and ventral rostral putamen [VRP]), and confirmed the differential connectivity of the associative, sensorimotor, and affective striatal subdivisions with the respective cortical regions.

Until the present time, an investigation into the connectivity of striatal subregions in different phases of BP has not been reported. The goal of this study was to investigate, for the first time, the differential connectivity of the striatal subregions in medication-free BPD and BPM groups compared with HCs. We hypothesized that both BPD and BPM would show striatal subregion connectivity abnormalities, and if these abnormalities were state specific, then they would be in the different directions in the two groups compared with the HC group, keeping in mind the differences in the motor, cognitive, and affective differences seen in the two states.

Materials and Methods

Subjects

BP patients who were medication-free for at least 2 weeks, along with HCs, were recruited from the outpatient psychiatry clinic at Indiana University Hospital and by advertisement to the community. After complete description of the study, written informed consent, approved by the Institutional Review Board (IRB) at the Indiana University School of Medicine, was obtained. All subjects signed an informed consent form. Both patients and HCs were paid $75 for screening and $75 for an MRI scan. Subjects underwent the Mini International Neuropsychiatric Interview (MINI) (Sheehan et al., 1998) as well as a clinical interview by a psychiatrist (A.A.) to determine the appropriate *Diagnostic and Statistical Manual 4th Edition Text Revision* (*DSM-IV-TR*) (First et al., 2002) diagnoses. Subjects were also rated on the 17-item Hamilton Depression Rating Scale (HAMD) (Hamilton, 1960) and Young Mania Rating Scale (YMRS) (Young et al., 1978) on the day of the scan.

BP participants aged 18–60 years were included in the study if they satisfied *DSM-IV-TR* criteria for BP and satisfied *DSM-IV-TR* criteria for (hypo)mania or a depressed episode. In addition, to further delineate the two BP groups, on the day of the scan, the BPD group was required to have HAMD ≥15 and YMRS ≤10 and the BPM group an HAMD ≤12 and a YMRS ≥12. Exclusion criteria for participants included the following: lifetime diagnosis of schizophrenia or schizoaffective disorder; a current primary anxiety disorder; use of psychotropic medications in the past 2 weeks; fluoxetine use over the past 4 weeks; acute suicidal or homicidal ideation or behavior; recent (<1 week) or current inpatient hospitalization; meeting *DSM-IV-TR* criteria for substance dependence within the past year, except nicotine; positive urinary toxicology screening at baseline; use of alcohol in the past 1 week; serious medical or neurological illness; current pregnancy or breast feeding; and metallic implants or other contraindications to MRI. HCs (18–60 years), besides satisfying the above exclusion criteria, had no personal or family history of psychiatric illness.

fMRI scan

Scans were performed using a Siemens 3T Tim Trio. After a short scout imaging scan to survey head position and center the field of view (FOV), a high- resolution three-dimensional magnetization prepared rapid gradient echo (MPRAGE) scan was collected (160 sagittal slices and $1.0 \times 1.0 \times 1.2$ mm voxel dimension). Resting-state scans were acquired with the following parameters: T2*-weighted, gradient echo, echo-planar imaging sequence TR/TE 2250/29 ms; 39 axial slices; FOV 220×220 mm; voxel dimension $2.5 \times 2.5 \times 3.5$ mm. An integrated

parallel acquisition technique was implemented using a generalized autocalibrating partially parallel acquisition (GRAPPA) with a reduction factor of 2 to improve spatial resolution, reduce geometric distortion, and decrease scan time. A resting-state 5-min 33 sec scan was acquired with 145 image volumes. Resting-state data were acquired while each subject was asked to lie awake with eyes closed and not think about anything in particular. After each resting-state scan was completed, the subjects were asked whether they were able to stay awake and comply with instructions. Scans during which subjects reported sleeping were not included in the analysis.

Image analysis

Preprocessing, including motion correction. The images were corrected for physiologic noise (Beall, 2010; Beall and Lowe, 2014; Glover et al., 2000) using signals obtained with PESTICA (Physiologic Estimation by Temporal Independent Component Analysis) (Beall and Lowe, 2007). Special attention was paid to motion correction because both linear and nonlinear motion artifacts have been shown to affect functional results (Power et al., 2012; Van Dijk et al., 2012). Motion correction was performed using SLice-Oriented MOtion COrrection (SLOMOCO) (Beall and Lowe, 2014). SLOMOCO first performs an in-plane slicewise motion registration, followed by an out-of-plane motion parameter estimation and regularization. The regularized out-of-plane and residual in-plane motion parameters are used in a slice-specific second-order motion model that accounts for the effect of adjacent slice motion into or out of the slice of interest as well as the present slice. Finally, the software regresses the physiologic noise model in parallel with the slicewise second-order motion model, and this regression correction comprises the last stage of SLOMOCO to produce data that have been corrected for physiologic noise and motion.

After motion correction, images were corrected for nonneural sources of variance using a regression-based correction with time series obtained from eroded white matter and ventricular masks (Jo et al., 2010). The corrected images were normalized to Montreal Neurological Institute (MNI) space, resampled to 2 mm isotropic voxels, and finally bandpass filtered to retain low-frequency fluctuations (0.008–0.08 Hz) using 3dBandpass from AFNI (Analysis of Functional Neuroimages) (Cox, 1996). For every scan, the number of motion-corrupted volumes was identified using the Jiang average voxel displacement measurement (Jiang et al., 1995) computed from the slicewise motion parameters from SLOMOCO. A corrupted volume was defined as a volume where at least one slice within that volume experienced >1 mm of out-of-plane motion. Any subject with 15 or more volumes with >1 mm of out-of-plane motion was excluded from the analysis (Beall and Lowe, 2014; Jiang et al., 1995). We selected 15 volumes as the cutoff because we had the goal for residual corruption to be in no more than 10% of the number of volumes acquired.

Seed reference regions. Twelve seed reference regions of interest (ROIs), 3.5 mm in radius, were made using the MNI coordinates (Table 1) as described previously (Di Martino et al., 2008). Of these regions, three of them were in the

TABLE 1. COORDINATES OF THE REFERENCE ROIs

ROI	Coordinates of the centers of ROIs (MNI)		
	X	Y	Z
VSI	±9	9	−8
VSS	±10	15	0
DC	±13	15	9
DCP	±28	1	3
DRP	±25	8	6
VRP	±20	12	−3

ROIs made with 3.5 mm radius (Di Martino et al., 2008).
DC, dorsal caudate; DCP, dorsal caudal putamen; DRP, dorsal rostral putamen; MNI, Montreal Neurological Institute; ROIs, regions of interest; VRP, ventral rostral putamen; VSI, ventral striatum inferior; VSS, ventral striatum superior.

caudate area (DC, VSS, and VSI) and three in the putamen area (DRP, DCP, and VRP).

First-level analysis for generation of connectivity maps. Mean of the time series of each ROI for each subject was extracted from the filtered preprocessed images. Next, functional connectivity maps were created for each reference region in Statistical Parametric Mapping version 8 (SPM8) (Penny et al., 2011) image analysis software, quantifying the correlation between the reference region time series and all other brain voxels. Subsequently, the connectivity maps from the first-level analysis were z transformed and smoothed with an 8-mm kernel, and then they were used for between-group second-level analyses.

Main effect analysis. A factorial second-level analysis model using group (BPD, BPM, and HC) as factor and age and gender as covariates was constructed in SPM8. The resultant main effect images were voxelwise thresholded at $Z > 2.3$, and a whole-brain cluster significance threshold of 0.004 (corrected) (0.05/12) was calculated at $k = 321$ using the 3dClustsim tool in AFNI. Significant areas were identified using the Automated Anatomical Labeling atlas (Rigucci et al., 2010).

Post hoc pairwise between-group analysis. To clarify and visualize between-group differences, connectivity beta coefficients from the significant clusters indicating main effects for each ROI (Table 3) were extracted and post hoc pairwise differences examined at $p = 0.05$ (Bonferroni corrected for the six pairwise group comparisons) using SPSS 21 (IBM Corp., 2012).

Correlation analysis connectivity. Beta coefficients were extracted from the significant main effect clusters of each ROI and, using SPSS, Pearson's correlation was calculated with the 17-item HAMD and YMRS scores within the combined BP group ($N = 60$ subjects). Significant correlations were identified after Bonferroni correction for the number of main effect clusters identified for each reference ROI. A separate within-group correlation analysis was conducted between functional connectivity and YMRS scores and functional connectivity and HAMD scores for BPM and BPD groups, respectively.

Results

Demographics and illness characteristics

A total of 75 participants with BP (BPD and BPM) were initially included in the study (Table 2). Of these, four subjects were excluded for not meeting the HAMD and YMRS ratings criteria, three subjects were excluded for unreliable or unclear history of illness or information, four subjects for motion, one subject reported briefly falling asleep, and one subject could not complete the scan. Of the remaining 62 BP subjects, close gender and age match was achieved across groups for 30 BPM and 30 BPD groups. The BP groups were then demographically matched with 30 HCs, and these participants were included in the final analysis. Table 2 summarizes the participants' demographic and clinical characteristics. As per recruitment criteria, the BPD group had significantly higher scores on the HAMD and the BPM group had higher scores on the YMRS. There were no significant differences among the two BP groups in terms of demographics and illness characteristics (Table 1). BPM and BPD were required to be medication-free at the time of inclusion for at least 2 weeks, but many were medication-free for much longer periods of time. BP patients were in the medication-free state because they did not want to take medication, had not followed up on treatment recommendations, or did not have insurance to get treatment. All but two of the BPM subjects were in the hypomanic state—this is expected as the subjects, despite not being on medications, presented as outpatients.

Within-group connectivity

Within-group results (voxelwise family-wise-error [FWE] corrected $p = 0.05$) for HCs showed results similar to that described by previously published studies (Di Martino et al., 2008; Postuma and Dagher, 2006) (see Supplementary Figs. S1–S6; Supplementary Data are available online at www.liebertpub.com/brain). DC showed significant connectivity to the dorsal and medial prefrontal cortex (MPFC). The VSI, which was situated in the nucleus accumbens area, showed expected connectivity with the pregenual and subgenual ACC. The VSS showed connectivity with the MPFC, medial and lateral orbitofrontal cortex (OFC), and the ACC. Similarly, the rostral putamen (DRP and VRP) showed significant connectivity with the medial frontal cortex, insula, and the ACC. The DCP showed connectivity with the sensorimotor regions, including the medial frontal cortex, parietal cortex, and the insula.

The main focus of this report is between-group results for BPD and BPM. Therefore, within-group results for BPD and BPM are only briefly presented here. Within-group results for BPD and BPM groups demonstrated some similarities to that of within-group results for HCs, in that for both BPD and BPM groups, there was significant DC connectivity to MPFC areas. For VSS and VSI connectivity, the BPD group showed connectivity to the inferior frontal gyrus where the BPM group showed VSS and VSI connectivity to medial-inferior frontal gyrus. For rostral putamen areas, BPM showed significant connectivity to middle frontal cortex areas as well as the brainstem and BPD showed connectivity to medial to inferior frontal areas and brainstem.

Between-group functional connectivity differences

Main effects of group. Main effects for group differences were seen for the left and right DC, VSI, VRP, and for the left DCP ($p = 0.004$, cluster-wise corrected) and are presented in Table 3. Main effects for group differences were seen for the left DC in the inferior frontal cortex (IFC) extending to the OFC and the insula. For the right DC, on the other hand, the main effect was seen in a midbrain area close to the substantia nigra. For the ventral affective striatum, main effects for the ventral VSI area were seen for the left and right ACC and thalamus, as well as a midbrain area extending to the olfactory cortex. For the left and right VRP, main effects of the

TABLE 2. CLINICAL AND DEMOGRAPHIC INFORMATION BY GROUP

Measures	BPD (N=30) Mean (SD)	BPM (N=30) Mean (SD)	HC (N=30) Mean (SD)	ANOVA
Age (years)	34 (11)	33 (11)	31 (10)	NS
Age at first episode (years)	16 (9)	15 (4)		NS
Hamilton Depression Rating Scale score (17 item)	20 (3)	6 (3)	0 (0)	0.001
Young Mania Rating score	2 (2)	16 (3)	0 (0)	0.001
	Mean (SD)	Mean (SD)		
Period off medication before scan (months)	28 (34)	49 (70)		NS
Number of prior mood episodes (depression)	>20	>20		
Number of prior mood episodes ((hypo)mania)	>20	>20		
Time since last manic episode (weeks)	25 (32)	28 (48)		NS
Time since last depressive episode (weeks)	35 (30)	36 (87)		NS
	N (%)	N (%)	N (%)	χ^2
Female	17 (57)	19 (63)	18 (60)	NS
Caucasian	25 (83)	28 (93)	28 (93)	NS
History of psychosis	11 (37)	8 (27)		NS
Bipolar I	12 (40)	16 (53)		
Bipolar II	18 (60)	14 (47)		NS
Past history of alcohol abuse	15 (50)	10 (33)		NS
Past history of drug abuse	13 (43)	13 (43)		NS
Right-handedness	19 (83)	22 (88)	27 (90)	NS

HC, healthy control; BPD, depression; BPM, (hypo)mania.

TABLE 3. MAIN EFFECTS OF GROUP (CLUSTERWISE SIGNIFICANCE OF $p=0.004$ [CORRECTED] AT $K=321$ AND VOXELWISE THRESHOLDED AT $Z>2.3$)

	Main effects of group						Significant post hoc results		
Reference region	Target cluster region	BA area	Cluster size	Peak Z	Peak p(unc)	Peak MNI	BPD vs. HC	BPM vs. HC	BPD vs. BPM
Left dorsal caudate	Left IFC extending to OFC and insula	45	1975	4.1	0	−32 36 10	BPD>HC	BPM>HC	
Right dorsal caudate	Midbrain around right substantia nigra		589	3.88	0	6 −16 −18		BPM>HC	BPM>BPD
Left ventral striatum inferior (ventral caudate/nucleus accumbens inferior)	Left and right anterior cingulate	24, 32	719	3.38	0	−4 42 16	BPD>HC	BPM>HC	
Right ventral striatum inferior (ventral caudate/nucleus accumbens inferior)	Midbrain extending to olfactory		666	3.84	0	10 4 −10	BPD>HC	BPM>HC	
	Right and left thalamus		611	3.81	0	2 −12 10	BPD>HC	BPM>HC	BPM>BPD
Left ventral rostral putamen	Left IFC extending to insula	45	644	4.24	0	−32 28 10	BPD>HC	BPM>HC	
	Left lingual gyrus extending to middle occipital gyrus	18	694	3.82	0	−30 −72 −2	BPD>HC	BPM>HC	
	Left precentral gyrus and postcentral gyrus	4, 3, 1, 2	397	3.52	0	−36 −32 66	BPD>HC		
	Right lingual gyrus	18	446	3.35	0	20 −50 −2	BPD>HC	BPM>HC	
Right ventral rostral putamen	Left IFC extending to insula	45	447	3.66	0	−38 28 2	BPD>HC	BPM>HC	
	Midbrain		400	3.65	0	0 −24 −12	BPD>HC	BPM>HC	
	Right superior temporal gyrus extending into insula	22, 41, 42	525	3.59	0	50 −2 0	BPD>HC		
Left dorsal caudal putamen	Right middle frontal gyrus	9, 10	602	5.37	0	50 22 42	HC>BPD	HC>BPM	
	Right superior medial frontal gyrus	10	383	4.16	0	4 36 54	HC>BPD	HC>BPM	
	Right superior temporal gyrus extending to insula	22, 41, 42	331	3.35	0	50 −4 10	BPD>HC		BPD>BPM

Post hoc significant results at $p=0.05$ (Bonferroni corrected for number of pairwise comparisons).
IFC, inferior frontal cortex; OFC, orbitofrontal cortex; BA, Brodmann's Area.
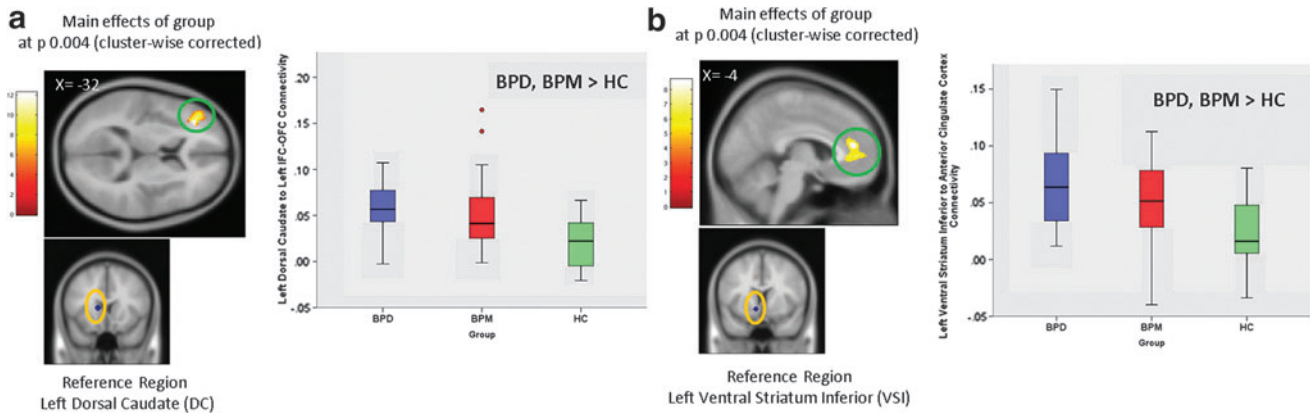
259

FIG. 1. Key differences found in both BPD (bipolar depressed) and BPM (hypo)manic) groups compared with the HC group. **(a)** *Post hoc* results of left DC connectivity to left IFC extending to inferior OFC (*p*=0.05 Bonferroni corrected for number of pairwise comparisons). **(b)** *Post hoc* results of left VSI connectivity to ACC (*p*=0.05 Bonferroni corrected). ACC, anterior cingulate cortex; DC, dorsal caudate; HC, healthy control; IFC, inferior frontal cortex; OFC, orbital frontal cortex; VSI, ventral striatum inferior. Color images available online at www.liebertpub.com/brain

group were seen in frontal and lingual gyri. For the left DCP, main effects were seen in the medial frontal areas, temporal gyri, and insula.

Pairwise differences. The beta coefficients extracted from the main effects of group areas were examined in

SPSS 21 to test for significant (*p*=0.05, Bonferroni corrected for number of pairwise comparisons) *post hoc* pairwise results (Figs. 1 and 2).

BPD versus HC, BPM. The BPD group, but not the BPM group, showed increased connectivity between the left VRP
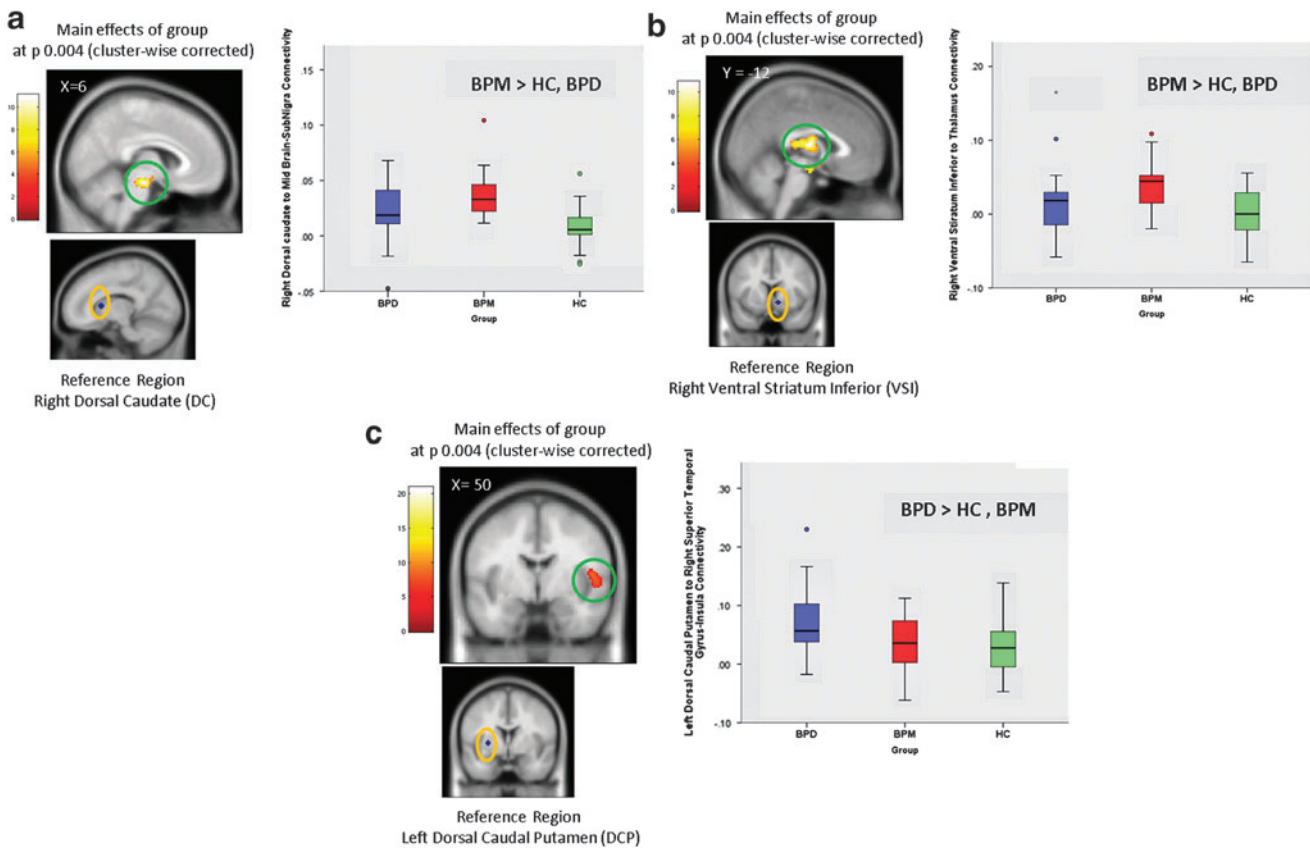

FIG. 2. Differences in either BPD (bipolar depressed) and BPM ((hypo)manic) groups compared with the HC group. **(a)** *Post hoc* results of right DC connectivity to midbrain-sub nigra (*p*=0.05 Bonferroni corrected for number of pairwise comparisons). **(b)** *Post hoc* results of right VSI connectivity to left and right thalamus (*p*=0.05 Bonferroni corrected for number of pairwise comparisons). **(c)** *Post hoc* results of left DCP connectivity to right superior temporal gyrus–insula (*p*=0.05 Bonferroni corrected for number of pairwise comparisons). DCP, dorsal caudal putamen. Color images available online at www.liebertpub.com/brain

and pre and postcentral frontal gyri (BPD>HC, $t=$ 4.638, $df=58$, $p<0.001$), as well as increased connectivity of the right VRP with the right superior temporal gyrus extending into the insula (BPD>HC, $t=3.426$, $df=46$, $p=$ 0.002). Finally, compared with both BPM and HCs, BPD connectivity was uniquely increased between left DCP and the right superior temporal gyrus extending to the insula (BPD>HC, $t=3.636$, $df=55$, $p=0.001$; BPD>BPM, $t=$ 2.892, $df=57$, $p=0.006$).

BPM versus BPD, HC. The BPM group exhibited unique increased connectivity compared with BPD as well as HCs in two caudate subregions. This increased connectivity was between right DC and midbrain around substantia nigra (BPM> BPD, $t=2.868$, $df=52$, $p=0.009$; BPM>HC, $t=6.189$, $df=57$, $p<0.001$) and between right VSI and bilateral thalamus (BPM>BPD, $t=2.320$, $df=55$, $p=0.05$; BPM>HC, $t=4.786$, $df=58$, $p<0.001$).

For the regional differences between BPM and BPD groups, the effect of bipolar subtype (I and II) was examined. No interaction effect of bipolar subtype and BP state was significant.

BPD, BPM versus HC. Pairwise results demonstrated that BPD and BPM connectivity was higher than HCs within most of the other main effect regions. This included left DC connectivity with the left IFC extending to OFC and insula (BPD>HC, $t=5.495$, $df=58$, $p<0.001$; BPM>HC, $t=3.803$, $df=52$, $p<0.001$), left VSI connectivity with bilateral ACC (BPD>HC, $t=4.630$, $df=53$, $p<0.001$; BPM>HC, $t=2.727$, $df=50$, $p=0.022$), and right VSI connectivity with midbrain/olfactory cortex (BPD>HC, $t=4.609$, $df=52$, $p<$ 0.001; BPM>HC, $t=4.858$, $df=55$, $p<0.001$). Both BPD and BPM had increased connectivity compared with HCs of left VRP connectivity with the left IFC extending to insula (BPD>HC, $t=3.389$, $df=52$, $p=0.004$; BPM>HC, $t=4.108$, $df=55$, $p=0.001$), left lingual gyrus extending to middle occipital gyrus (BPD>HC, $t=4.238$, $df=48$, $p<0.001$; BPM> HC, $t=3.461$, $df=49$, $p=0.008$), and the right lingual gyrus (BPD>HC, $t=3.670$, $df=53$, $p=0.002$; BPM>HC, $t=$ 3.199, $df=54$, $p=0.014$), and of the right VRP with the left IFC extending to insula (BPD>HC, $t=3.515$, $df=57$, $p=0.001$; BPM>HC, $t=3.874$, $df=58$, $p=0.001$), and midbrain areas (BPD>HC, $t=3.564$, $df=51$, $p=0.002$; BPM> HC, $t=4.866$, $df=53$, $p<0.001$). On the other hand, left DCP connectivity with the right middle frontal gyrus (HC> BPD, $t=4.440$, $df=53$, $p<0.001$; HC>BPM, $t=3.765$, $df=54$, $p<0.001$) and medial frontal cortex (HC>BPD, $t=4.411$, $df=57$, $p<0.001$; HC>BPM, $t=3.748$, $df=58$, $p=0.01$) was higher in HCs compared with both BPD and BPM groups.

Correlation analysis

Correlation with YMRS and HAMD (Bonferroni corrected for number of main effect target regions for each reference ROI; Table 3) was investigated: Right DC-substantia nigra connectivity was positively correlated with YMRS scores (r: 0.297, $p=0.02$ [corrected]) and negatively correlated with HAMD scores (r: -0.386, $p=0.002$ [corrected]). On the other hand, left DCP-right superior temporal gyrus had positive correlation with the HAMD scores (r: 0.347,

$p=0.007$ [corrected]). Because the main effect regions, which showed abnormality in the same direction for both BPD and BPM, did not show any correlation with HAMD or YMRS, the correlation results listed above are likely to reflect group differences in functional connectivity.

In the separate correlation analysis between clinical measures and functional connectivity within each group, there was no significant correlation between connectivity measures and HAMD scores in the BPD group and no significant correlation between connectivity measures and YMRS scores in the BPM group (Fig. 3).

Discussion

In accord with our hypotheses, both BPD and BPM exhibited striatal subregion connectivity abnormalities. As we had hypothesized, differences were seen between BPM and BPD and these findings are likely to be state related. Two putamen regions showed unique increased connectivity in BPD and two caudate subregions showed unique increased connectivity in BPM compared with BPD and HC.

Two putamen subregions exhibited unique increased connectivity in the BPD group. BPD, but not the BPM, group showed increased right VRP connectivity to right superior temporal gyrus extending to the insula compared with HCs. BPD also showed increased connectivity of the left DCP with the right superior temporal gyrus extending to insula compared with both HC and BPM groups.

The putamen plays an important role in correlation of motor functions. Studies that investigated functions of striatal subregions also showed the involvement of putamen in executive and somatosensory regions (Di Martino et al., 2008). The VRP is part of the associative/cognitive striatum (Di Martino et al., 2008; Postuma and Dagher, 2006). Its increased connectivity with the temporal gyrus and insula in BPD may signify changes in emotional interpretation of negative thoughts and cognitive changes in depressed states. The anterior insula has been implicated in monitoring of cognitive and autonomic responses to emotional stimuli (Augustine, 1996; Craig, 2009; Elliott et al., 2000; George et al., 1998; Wessa et al., 2007) and is an important component of the so-called salience network, which monitors the internal state of the organism. The greater connectivity of the insula to VRP in BPD (vs. HC) may reflect abnormalities in the salience network. The DCP is part of the somatosensory striatum and its increased connectivity with the temporal gyrus and insula may be related to increased salience of internal and external negative events seen in depression.

The caudate is an integral part of cortical and subcortical feedback loops, which control motivation and behavior. In particular, the caudate-cortical loop is thought to be involved in monitoring of outcome of action and therefore integral to control of motivation and behavior (Postuma and Dagher, 2006). The DC is thought to be part of the associative/cognitive striatum as it connects with associative cortical structures such as the prefrontal cortex. Increased right DC connectivity to midbrain near the right substantia nigra (a dopamine-rich area) may signify a greater dopaminergic functional input to this area, leading to increased activity of the caudate-cortical loop, which may underlie the abnormalities of monitoring outcome of behavior in BPM. The second caudate area, which showed increased connectivity
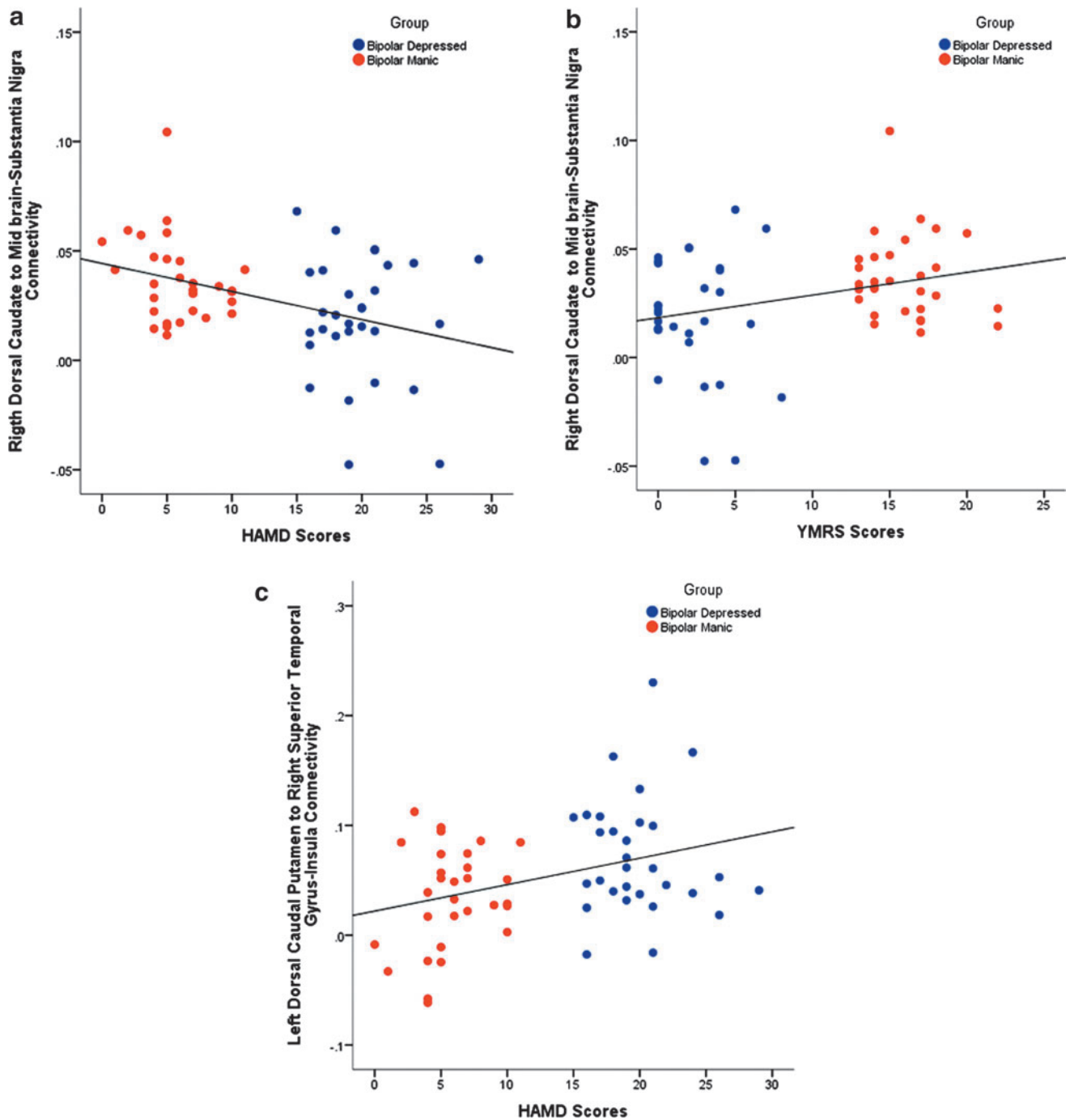
FIG. 3. Correlation analysis between the increase in connectivity and change in Symptom Severity Scales (Bonferroni corrected for number of main effect target regions for each reference ROI). **(a)** Correlation between right DC with substantia nigra connectivity and HAMD Scores (r: -0.386, $p = 0.002$ [corrected]). **(b)** Correlation between right DC with substantia nigra connectivity and YMRS scores (r: 0.297, $p = 0.02$ [corrected]). **(c)** Correlation between left DCP with right superior temporal gyrus–insula connectivity and HAMD Scores (r: 0.347, $p = 0.007$ [corrected]). HAMD, Hamilton Depression Rating Scale; ROI, region of interest; YMRS, Young Mania Rating Scale. Color images available online at www.liebertpub.com/brain

in BPM, was the right VSI, which exhibited increased connectivity with the right and left thalamus. The VSI is part of the nucleus accumbens, which is involved in reward-related behavior and sends output through the ventral palladium to the thalamus. Increased reward seeking is an important symptom of (hypo)mania and therefore it is not surprising that its connectivity is increased with the thalamus, which

acts as a relay between cortical and subcortical structures. In summary, dorsal and ventral caudate abnormalities seen predominantly in BPM may reflect the abnormalities of motivation and reward-seeking behavior in the (hypo)manic state.

As hypothesized, BPD and BPM also exhibited several abnormalities that were common to both BPD and BPM

compared with HCs (Table 3). The similar abnormalities in BPD and BPM versus HCs did not correlate with HAMD or YMRS scores. Therefore, these abnormalities could either be interpreted as being trait related or mood state nonspecific, that is, these abnormalities are related to an abnormal mood state regardless of valence. A number of previous studies, which have examined activation and connectivity abnormalities concurrently in mania and depression, have also uncovered many similar findings in both BPM and BPD (Anand et al., 2009; Chen et al., 2006; Hulvershorn et al., 2012; Hummer et al., 2013; Marchand et al., 2007a; Phillips and Swartz, 2014; Wessa et al., 2007). To definitely ascertain that these abnormalities are trait related, they need to be investigated in medication-free euthymic subjects in future studies.

The associative striatal areas such as DC and VRP showed increased connectivity with the frontal cortical regions, including the IFC. The limbic striatal areas, VSI and VSS, showed increased connectivity with associated limbic areas such as the ACC and the midbrain involved in emotional expression. For the sensorimotor striatal area of left DCP, on the other hand, HCs showed increased connectivity compared with both BPD and BPM. As these abnormalities did not show a correlation with either the YMRS or the HAMD they are likely to be trait related and may underlie the cognitive, motor, and affective abnormalities that have been reported in euthymic BP (Adler et al., 2004; Caligiuri et al., 2006; Marchand et al., 2007b; Wessa et al., 2007).

The above findings and their interpretation need to be considered in the context of the limitations of the study. The ROI-based approach used in this study has the advantage of being based on *a priori* hypotheses generated from previous neuroanatomical and neuroimaging studies. Consequently, the findings are much more interpretable in terms of regional neuronal connection differences between groups (Greicius, 2008). However, other regions of importance may be neglected with this method. Alternative methods such as graph theory-based analysis (Bullmore and Sporns, 2009) and ICA-based multiple brain networks analysis (Beckmann et al., 2005) could also be applied to the data in the future to conduct a more discovery-based exploration of brain networks in BP.

Motion-related artifacts have been of particular concern in resting-state functional analyses (Van Dijk et al., 2012). As detailed under the Image Analysis section, several measures were taken to account for these artifacts. Furthermore, the motion criteria used to include subjects went beyond what is typically used in analyses that rely on frame removal.

Although the findings of this study are not confounded by concurrent use of medication, long-term effects of past use of medications cannot be fully ruled out. BPM subjects were mostly hypomanic, but were clearly in a mood elevated state compared with the BPD group, as evidenced by the ascertainment of their *DSM-IV* diagnosis using a structured interview and subsequent HAMD and YMRS ratings. Patients judged to be in mixed states by *DSM-IV* criteria were not included in the study. Furthermore, there was a strong negative correlation between the HAMD and YMRS scores, an indirect evidence that patients were either in a predominantly (hypo)manic or depressed state. It is possible that more severely depressed or manic inpatient subjects may show wider separation of abnormalities between the BPD and BPM; however, these groups are likely to be imaged while on medications of different types, making the interpretation of the findings more difficult. The findings of this study should be compared with findings from the more severely ill subjects in the future to further elucidate the striatal connectivity abnormalities in BP.

As mentioned in the Results section, a separate correlation analysis was conducted between functional connectivity and clinical measures separately for each group—for the BPM group with YMRS scores and for the BPD group with HAMD scores. None of the results were found to be significant at a corrected level. This finding was possibly caused by the narrow range of scores and a small number of subjects within each group.

As we did not include a bipolar euthymic group in this analysis, it is difficult to tease out trait versus state-related findings. Nevertheless, findings that were markedly different from between the BPM and BPD groups are likely to be state related. Studies of all three phases and more than one phase, preferably within the same subject, need to be conducted to more definitively tease out state versus trait differences. We also examined the effect of bipolar subtype and the BP subtype did not have any effects on the results. However, future studies need to be conducted with matched BPI and BPII subjects to clarify effects of bipolar subtype on connectivity.

In conclusion, the findings of this study identified several abnormalities unique to the BPM and BPD states and many others, which were similar in both groups, signifying possible trait-related findings in BP.

Acknowledgment

Author Disclosure Statement

No competing financial interests exist.

References

Adler CM, Holland SK, Schmithorst V, Tuchfarber MJ, Strakowski SM. 2004. Changes in neuronal activation in patients with bipolar disorder during performance of a working memory task. Bipolar Disord 6:540–549.

Alexander GE, DeLong MR, Strick PL. 1986. Parallel organization of functionally segregated circuits linking basal ganglia and cortex. Annu Rev Neurosci 9:357–381.

Alheid GF, Heimer L. 1988. New perspectives in basal forebrain organization of special relevance for neuropsychiatric disorders: the striatopallidal, amygdaloid, and corticopetal components of substantia innominata. Neuroscience 27:1–39.

Anand A, Li Y, Wang Y, Lowe MJ, Dzemidzic M. 2009. Resting state corticolimbic connectivity abnormalities in unmedicated bipolar disorder and unipolar depression. Psychiatry Res 171:189–198.

Augustine JR. 1996. Circuitry and functional aspects of the insular lobe in primates including humans. Brain Res Brain Res Rev 22:229–244.

Beall EB. 2010. Adaptive cyclic physiologic noise modeling and correction in functional MRI. J Neurosci Methods 187:216–228.

Beall EB, Lowe MJ. 2007. Isolating physiologic noise sources with independently determined spatial measures. Neuroimage 37:1286–1300.

Beall EB, Lowe MJ. 2014. SimPACE: generating simulated motion corrupted BOLD data with synthetic-navigated acquisition for the development and evaluation of SLOMOCO: a new, highly effective slicewise motion correction. Neuroimage 101:21–34.

Beckmann CF, DeLuca M, Devlin JT, Smith SM. 2005. Investigations into resting-state connectivity using independent component analysis. Philos Trans R Soc Lond B Biol Sci 360: 1001–1013.

Berendse HW, Galis-de Graaf Y, Groenewegen HJ. 1992. Topographical organization and relationship with ventral striatal compartments of prefrontal corticostriatal projections in the rat. J Comp Neurol 316:314–347.

Bigler ED, Mortensen S, Neeley ES, Ozonoff S, Krasny L, Johnson M, Lu J, Provencal SL, McMahon W, Lainhart JE. 2007. Superior temporal gyrus, language function, and autism. Dev Neuropsychol 31:217–238.

Bullmore E, Sporns O. 2009. Complex brain networks: graph theoretical analysis of structural and functional systems. Nat Rev Neurosci 10:186–198.

Caligiuri MP, Brown GG, Meloy MJ, Eberson S, Niculescu AB, Lohr JB. 2006. Striatopallidal regulation of affect in bipolar disorder. J Affect Disord 91:235–242.

Carpenter MB. 2011. Anatomy of the Corpus Striatum and Brain Stem Integrating Systems. Uniformed Services University of the Health Sciences: Bethesda, Maryland. Compr Physiol: 947–995.

Chen CH, Lennox B, Jacob R, Calder A, Lupson V, Bisbrown-Chippendale R, Suckling J, Bullmore E. 2006. Explicit and implicit facial affect recognition in manic and depressed states of bipolar disorder: a functional magnetic resonance imaging study. Biol Psychiatry 59:31–39.

Cox RW. 1996. AFNI: software for analysis and visualization of functional magnetic resonance neuroimages. Comput Biomed Res 29:162–173.

Craig AD. 2009. How do you feel—now? The anterior insula and human awareness. Nat Rev Neurosci 10:59–70.

DeLong, MR and Georgopoulos, AP. 2011. Motor Functions of the Basal Ganglia. The Johns Hopkins University School of Medicine: Baltimore, Maryland. Compr Physiol; 1017–1061.

Di Martino A, Scheres A, Margulies DS, Kelly AM, Uddin LQ, Shehzad Z, Biswal B, Walters JR, Castellanos FX, Milham MP. 2008. Functional connectivity of human striatum: a resting state FMRI study. Cereb Cortex 18:2735–2747.

Elliott R, Rubinsztein JS, Sahakian BJ, Dolan RJ. 2000. Selective attention to emotional stimuli in a verbal go/no-go task: an fMRI study. Neuroreport 11:1739–1744.

First MB, Frances A, Pincus HA. 2002. DSM-IV-TR Handbook of Differential Diagnosis. American Psychiatric Publishing, Inc.: Arlington, VA.

George MS, Huggins T, McDermut W, Parekh PI, Rubinow D, Post RM. 1998. Abnormal facial emotion recognition in depression: serial testing in an ultra-rapid-cycling patient. Behav Modif 22:192–204.

Glover GH, Li TQ, Ress D. 2000. Image-based method for retrospective correction of physiological motion effects in fMRI: RETROICOR. Magn Reson Med 44:162–167.

Goldman PS, Nauta WJ. 1977. An intricately patterned prefronto-caudate projection in the rhesus monkey. J Comp Neurol 72:369–386.

Greicius M. 2008. Resting-state functional connectivity in neuropsychiatric disorders. Curr Opin Neurol 21:424–430.

Haber SN, Lynd E, Klein C, Groenewegen HJ. 1990. Topographic organization of the ventral striatal efferent projections in the rhesus monkey: an anterograde tracing study. J Comp Neurol 293:282–298.

Hamilton M. 1960. A rating scale for depression. J Neurol Neurosurg Psychiatry 23:56–62.

Hulvershorn LA, Karne H, Gunn AD, Hartwick SL, Wang Y, Hummer TA, Anand A. 2012. Neural activation during facial emotion processing in unmedicated bipolar depression, euthymia, and mania. Biol Psychiatry 71:603–610.

Hummer TA, Hulvershorn LA, Karne HS, Gunn AD, Wang Y, Anand A. 2013. Emotional response inhibition in bipolar disorder: a functional magnetic resonance imaging study of trait- and state-related abnormalities. Biol Psychiatry 73: 136–143.

IBM Corp. 2012. IBM SPSS Statistics for Windows. Armonk, NY: IBM Corp.

Jiang A, Kennedy DN, Baker JR, Weisskoff RM, Tootell RBH, Woods RP, Benson RR, Kwong KK, Brady TJ, Rosen BR, Belliveau JW. 1995. Motion detection and correction in functional MR imaging. Hum Brain Mapp 3:224–235.

Jo HJ, Saad ZS, Simmons WK, Milbury LA, Cox RW. 2010. Mapping sources of correlation in resting state FMRI, with artifact detection and removal. Neuroimage 52: 571–582.

Kemp JM, Powell TP. 1971. The connexions of the striatum and globus pallidus: synthesis and speculation. Philos Trans R Soc Lond B Biol Sci 262:441–457.

Kunzle H. 1975. Bilateral projections from precentral motor cortex to the putamen and other parts of the basal ganglia. An autoradiographic study in Macaca fascicularis. Brain Res 88: 195–209.

Liles SL, Updyke BV. 1985. Projection of the digit and wrist area of precentral gyrus to the putamen: relation between topography and physiological properties of neurons in the putamen. Brain Res 339:245–255.

Marchand WR, Lee JN, Thatcher GW, Jensen C, Stewart D, Dilda V, Thatcher J, Creem-Regehr SH. 2007a. A functional MRI study of a paced motor activation task to evaluate frontal-subcortical circuit function in bipolar depression. Psychiatry Res 155:221–230.

Marchand WR, Lee JN, Thatcher J, Thatcher GW, Jensen C, Starr J. 2007b. A preliminary longitudinal fMRI study of frontal-subcortical circuits in bipolar disorder using a paced motor activation paradigm. J Affect Disord 103:237–241.

Marchand WR, Yurgelun-Todd D. 2010. Striatal structure and function in mood disorders: a comprehensive review. Bipolar Disord 12:764–785.

Penny WD, Friston KJ, Ashburner JT, Kiebel SJ, Nichols TE. 2011. Statistical Parametric Mapping: The Analysis of Functional Brain Images. Academic Press: Cambridge, MA.

Phelps PE, Vaughn JE. 1986. Immunocytochemical localization of choline acetyltransferase in rat ventral striatum: a light and electron microscopic study. J Neurocytol 15:595–617.

Phillips ML, Swartz HA. 2014. A critical appraisal of neuroimaging studies of bipolar disorder: toward a new conceptualization of underlying neural circuitry and a road map for future research. Am J Psychiatry 171:829–843.

Postuma RB, Dagher A. 2006. Basal ganglia functional connectivity based on a meta-analysis of 126 positron emission tomography and functional magnetic resonance imaging publications. Cereb Cortex 16:1508–1521.

Power JD, Barnes KA, Snyder AZ, Schlaggar BL, Petersen SE. 2012. Spurious but systematic correlations in functional connectivity MRI networks arise from subject motion. Neuroimage 59:2142–2154.

Price JL, Drevets WC. 2010. Neurocircuitry of mood disorders. Neuropsychopharmacology 35:192–216.

Ragsdale CW, Jr., Graybiel AM. 1981. The fronto-striatal projection in the cat and monkey and its relationship to inhomogeneities established by acetylcholinesterase histochemistry. Brain Res 208:259–266.

Rigucci S, Serafini G, Pompili M, Kotzalidis GD, Tatarelli R. 2010. Anatomical and functional correlates in major depressive disorder: the contribution of neuroimaging studies. World J Biol Psychiatry 11:165–180.

Russchen FT, Bakst I, Amaral DG, Price JL. 1985. The amygdalostriatal projections in the monkey. An anterograde tracing study. Brain Res 329:241–257.

Sheehan DV, Lecrubier Y, Sheehan KH, Amorim P, Janavs J, Weiller E, Hergueta T, Baker R, Dunbar GC. 1998. The Mini-International Neuropsychiatric Interview (M.I.N.I.): the development and validation of a structured diagnostic psychiatric interview for DSM-IV and ICD-10. J Clin Psychiatry 59 Suppl 20:22–33;quiz 34–57.

Strakowski SM, Delbello MP, Adler CM. 2005. The functional neuroanatomy of bipolar disorder: a review of neuroimaging findings. Mol Psychiatry 10:105–116.

Teng S, Lu CF, Wang PS, Li CT, Tu PC, Hung CI, Su TP, Wu YT. 2014. Altered resting-state functional connectivity of striatal-thalamic circuit in bipolar disorder. PLoS One 9:e96422.

Townsend J, Altshuler LL. 2012. Emotion processing and regulation in bipolar disorder: a review. Bipolar Disord 14:326–339.

Van Dijk KR, Sabuncu MR, Buckner RL. 2012. The influence of head motion on intrinsic functional connectivity MRI. Neuroimage 59:431–438.

Vargas C, López-Jaramillo C, Vieta E. 2013. A systematic literature review of resting state network—functional MRI in bipolar disorder. J Affect Disord 150:727–735.

Wessa M, Houenou J, Paillère-Martinot M-L, Berthoz S, Artiges E, Leboyer M, Martinot J-L. 2007. Fronto-striatal overactivation in euthymic bipolar patients during an emotional go/nogo task. Am J Psychiatry 164:638–646.

Wessa M, Kanske P, Linke J. 2014. Bipolar disorder: a neural network perspective on a disorder of emotion and motivation. Restor Neurol Neurosci 32:51–62.

Young R, Biggs J, Ziegler V, Meyer D. 1978. A rating scale for mania: reliability, validity and sensitivity. Br J Psychiatry 133:429–435.

Address correspondence to:
Amit Anand
Center for Behavioral Health
Cleveland Clinic
9500 Euclid Avenue P57
Cleveland, OH 44122

E-mail: ananda@ccf.org